

- [14] Average of three samples for surface **1**, average of two samples for surface **2**.  
 [15] E. J. Lee, J. S. Ha, M. J. Sailor, *J. Am. Chem. Soc.* **1995**, *117*, 8295–8296.  
 [16] Resolution as observed through a microscope at 30 times magnification.  
 [17] T. Bischoff, G. Müller, W. Welser, F. Koch, *Sens. Actuators A* **1997**, *60*, 228–234.  
 [18] L. J. Bellamy, *The Infra-Red Spectra of Complex Molecules*, Methuen, New York, **1960**, p. 13.  
 [19] a) R. Walsh, *Acc. Chem. Res.* **1981**, *14*, 246–252; b) J. M. Kanabus-Kaminska, J. A. Hawari, D. Griller, C. Chatgililoglu, *J. Am. Chem. Soc.* **1987**, *109*, 5267–5268; c) C. Chatgililoglu, *Acc. Chem. Res.* **1992**, *25*, 188–194.  
 [20] J. L. Heinrich, A. Lee, M. J. Sailor, *Mater. Res. Soc. Symp. Proc.* **1995**, *358*, 605–610.  
 [21] O. Y. Okhlobystin, N. T. Berberova, *Dokl. Akad. Nauk. SSSR* **1993**, *332*, 599–600.  
 [22] The low incorporation observed at 650 nm is presumably almost exclusively a result of reaction with dangling bonds (ref. [20]) although migration of photogenerated excitons from the bulk into the porous layer may occur to a small extent: V. V. Doan, R. M. Penner, M. J. Sailor, *J. Phys. Chem.* **1993**, *97*, 4505–4508.  
 [23] R. P. S. Thakur, R. Singh, *Appl. Phys. Lett.* **1994**, *64*, 327–329.  
 [24] Y. H. Ogata, F. Kato, T. Tsuboi, T. Sakka, *J. Electrochem. Soc.* **1998**, *145*, 2439–2444.

## Cross-Section Molecular Imaging of Supramolecular Microtubes with Contact Atomic Force Microscopy

Toshimi Shimizu,\* Satomi Ohnishi, and Masaki Kogiso

Scanning probe microscopies, especially atomic force microscopy (AFM), are useful methods for obtaining molecularly resolved images of orientation and ordering in organic self-assemblies.<sup>[1, 2]</sup> In particular, AFM has been used to study two-dimensional, ordered organic molecules adsorbed on well-defined surfaces and at interfaces.<sup>[3]</sup> While there is an increasing number of studies on AFM imaging of biological macromolecules,<sup>[4–6]</sup> only a few reports<sup>[7–10]</sup> have described the morphologies and molecular orientation for synthetic supramolecular assemblies. However, no definitive information on these assemblies, especially along the molecular long axes, has been obtained at molecular resolution by AFM. Meanwhile, supramolecular self-organized fibers and their molecular arrangements have expertly been investigated with scanning and transmission electron microscopy.<sup>[11–13]</sup> We recently studied hydrogen bond directed self-assembly of chiral fibers<sup>[14]</sup> and microtubes<sup>[10, 15, 16]</sup> from synthetic sugar- and peptide-based bolaamphiphiles.<sup>[17]</sup> In light of the wide applicability of AFM, we explored vertical profiles along the molecular long

axes within the microtube<sup>[15]</sup> made up of glycyglycine bolaamphiphile **1**. Here we report a molecularly resolved layered structure within the tube membranes that was observed by contact AFM in air.

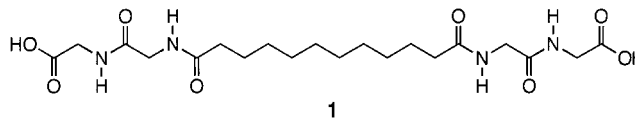


Figure 1 a shows a nonfiltered AFM image ( $19\ \mu\text{m} \times 19\ \mu\text{m}$ ) of supramolecular vesicle-encapsulated microtubes made up of **1**. We can observe a clear image similar to that obtained with phase-contrast and dark-field light microscopies (Figure 1 b). Spherical, brighter portions (denoted by arrows in Figure 1 a) correspond to topographically higher regions, and

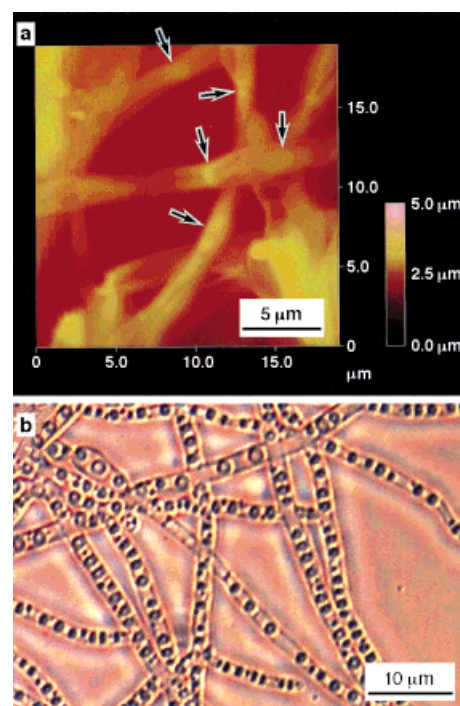


Figure 1. a) AFM height image ( $19\ \mu\text{m} \times 19\ \mu\text{m}$ ) of vesicle-encapsulated microtubes (denoted by arrows) made up of **1** and b) phase-contrast light micrograph of the microtubes (at  $25^\circ\text{C}$  in water).

indicate the encapsulation of vesicular assemblies in the compartment.<sup>[15]</sup> Cross-section analysis of the portions with and without vesicle encapsulation provided information on the thickness of the tube membranes; the value of less than 100 nm corresponds to less than 30–40 molecular layers.<sup>[10]</sup> In addition, a high-resolution AFM image of the tube surfaces also revealed a distorted hexagonal arrangement of the peptide head groups.<sup>[10]</sup> These findings indicate that AFM is a very useful tool for studying the molecular packing as well as the morphological dimensions of supramolecular assemblies.

The surface morphology of one tube is shown in Figure 2. The AFM image ( $1.45\ \mu\text{m} \times 1.45\ \mu\text{m}$ ) revealed a crack in the tube membrane. One can see a number of domains arranging like scales of a fish on the top of the tube as well as rodlike

[\*] Dr. T. Shimizu, Dr. S. Ohnishi, M. Kogiso  
 National Institute of Materials and Chemical Research  
 1–1 Higashi, Tsukuba, Ibaraki 305–8565 (Japan)  
 Fax: (+81) 298-54-4422  
 E-mail: tshimz@ccmail.nimc.go.jp

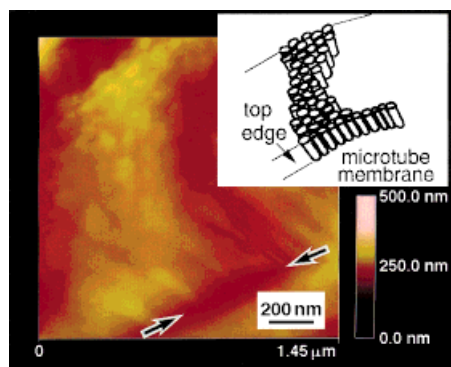


Figure 2. AFM height image ( $1.45\ \mu\text{m} \times 1.45\ \mu\text{m}$ ) of the microtube and the schematic illustration of the scalelike domains on the top and rodlike domains at the edge of the tube. A crack in the tube membrane is denoted by the arrows.

domains aligned parallel to the crack. The surfaces seem to have no homogeneous crystalline order on the micrometer scale. The diameters of the domains on the top of the tube are 20–100 nm, which agree well with the widths of the rodlike domains at the edge. This implies that columnar domains randomly assemble to construct the tube membranes (Figures 3a and 3b). Therefore, a high-resolution AFM image of the edge of the tube can be expected to directly provide

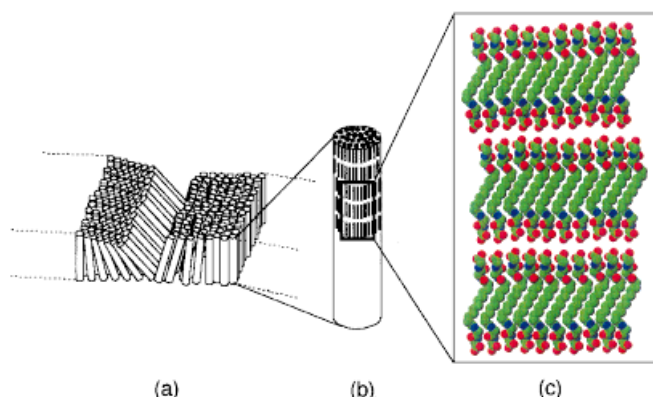


Figure 3. a) Microtube membrane composed of a number of columnar domains (b). c) A possible molecular alignment within a columnar domain.

information on the vertical molecular arrangement within the columnar domains. Such a crack in the tube membrane was frequently observed for this microtube. It occurs upon drying, not by deformation or damage due to interaction between the AFM tips and the tube membranes. The validity of this interpretation is supported by the AFM investigation in water. The dried microtubes swelled up again and exhibit no cracks when exposed to aqueous solution.

Figure 4 displays a high-resolution AFM image (friction mode,  $8\ \text{nm} \times 8\ \text{nm}$ ) for the edge of the tube. The image revealed parallel rows with a spacing of approximately 0.44–0.50 nm. We always observed the same molecular orientation and alignment, regardless of the image position and scanning speed. One can see two brighter zones separated by a distance of 2.9–3.2 nm. Considering the bola structure of **1**, the layered brighter zone was assigned to a terminal peptide head groups.

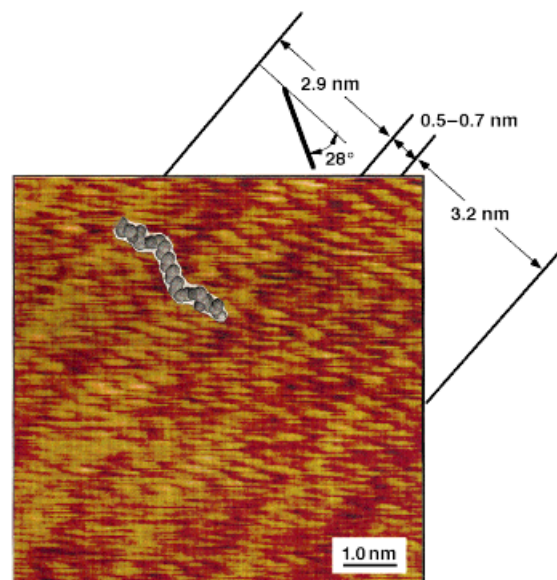


Figure 4. High-resolution AFM friction image ( $8.0\ \text{nm} \times 8.0\ \text{nm}$ ) of the edge of the tube.

In the AFM image, we can also find darker striations which correspond to the alkyl spacers. They align with their oligomethylene axes oriented at approximately  $28^\circ$  with respect to the normal of the layer plane. The image clearly shows that bolaamphiphilic molecules adopt a bent conformation at each end of the alkylene chain (Figure 3c). Relatively darker images at the middle of the molecules stem from smaller molecular volumes of the methylene group as compared with those of the peptide head groups. The observed features are in good accord with that in the crystal lattice (*ac* plane) of the same molecule.<sup>[18]</sup> Alternatively, we might be able to assign the layer zone to two sets of peptide head groups of neighboring layers adjacent to each other. The bolaamphiphilic molecules should then require crystalline dense packing through interlayer acid–acid hydrogen-bond formation. Furthermore, the evaluated molecular length ( $1.9 \pm 0.1\ \text{nm}$ ) for this model is too short with respect to that obtained for the single crystal (2.72 nm). Therefore, the possibility of this molecular arrangement would be ruled out.

The distance between two head groups of neighboring layers varies from 0.5 to 0.7 nm. This finding implies that intralayer interactions rather than interlayer interactions determine the supramolecular tube structure. This also suggests the predominance of intralayer acid–anion hydrogen-bond networks in the microtube, as supported by FT-IR studies.<sup>[10, 15]</sup> Interlayer interactions between the head groups will enforce crystalline order to form a three-dimensional crystal.<sup>[16, 18]</sup> Only one single-crystal analysis has been so far reported for a long-chain carboxylate with a potassium cation.<sup>[19]</sup> The carboxylate groups of potassium palmitate face each other with a distance of approximately 0.3 nm. Therefore, the soap crystal sheet is extremely slippery due to the rejection of the charged carboxylate groups.<sup>[20]</sup> A similar situation can be imaged for the bolaamphiphile sheet within the supramolecular tube membranes by AFM. Actually, the monolayered sheets of **1** seems to be slightly distorted to form

a rippled structure. It has a good resemblance to the  $P_\beta$  phase observed for lecithin–water phases.<sup>[21]</sup>

In conclusion, by contact AFM we directly observed for the first time a hierarchical formation of structures (bent molecule–distorted layer–columnar domain) as a vertical profile of the microtube membranes.

### Experimental Section

Supramolecular vesicle-encapsulated microtubes were prepared with a weak alkaline aqueous solution of glycylglycine bolaamphiphile **1** (10 mM, pH  $\approx$  8).<sup>[10]</sup> The formation of microtubes with uniform diameter (1.5–2.2  $\mu$ m) was confirmed by phase-contrast and dark-field light microscopy (Figure 1b). Droplets (20–30  $\mu$ L) of the solution containing the microtubes were placed with a pipette on to a clean glass substrate (Matsunami micro slide glass, precleaned, S-1111) and allowed to air-dry slowly (14 h) in an electric desiccator (Toyo Living auto dry, type FHO, humidity  $15 \pm 5\%$ ). All AFM measurements were performed with a commercial atomic force microscope (Digital Instruments Inc., Santa Barbara, CA, Nanoscope IIIa) at room temperature in air. We used the contact-mode AFM with a microfabricated silicon nitride cantilever (spring constant 0.12 N m<sup>-1</sup>). Images were recorded in the height or friction mode.

Received: May 5, 1998 [Z 11821 IE]

German version: *Angew. Chem.* **1998**, *110*, 3509–3511

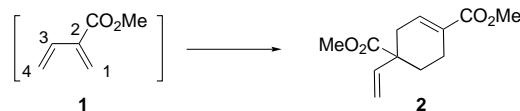
**Keywords:** amphiphiles • atomic force microscopy • hydrogen bonds • nanostructures • supramolecular chemistry

- [1] H. G. Hansma, S. A. C. Gould, P. K. Hansma, *Langmuir* **1991**, *7*, 1051–1054.
- [2] J. Y. Josefowicz, N. C. Maliszewski, S. H. J. Idziak, P. A. Heiney, J. P. McCauley, A. B. Smith III, *Science* **1993**, *260*, 323–326.
- [3] S. Chiang in *Scanning Tunneling Microscopy I* (Eds.: R. Wiesendanger, H. J. Guntherodt), Springer, Berlin, **1991**, p. 181.
- [4] S. M. Lindsay in *Scanning Tunneling Microscope and Spectroscopy* (Ed.: D. A. Donned), VCH, New York, **1992**, p. 335.
- [5] E. T. Kool, P. K. Hansma, M. Kashlev, S. Kasas, N. H. Thomson, B. L. Smith, H. G. Hansma, X. Zhu, M. Guthold, C. Bustamante, *Biochemistry* **1997**, *36*, 461–468.
- [6] C. Bustamante, G. Zuccheri, S. H. Leuba, G. Yang, B. Samori, *Methods* **1997**, *12*, 73–83.
- [7] I. Tuzov, K. Cramer, B. Pfannemuller, W. Kreutz, S. N. Magonov, *Adv. Mater.* **1995**, *7*, 656–659.
- [8] K. Craemer, S. Demharter, R. Muelhaupt, H. Frey, S. N. Magonov, I. Tuzov, M.-H. Whangbo, *New J. Chem.* **1996**, *20*, 5–11.
- [9] K. Ariga, N. Yamada, M. Naito, E. Koyama, Y. Okahata, *Chem. Lett.* **1998**, 493–494.
- [10] M. Kogiso, S. Ohnishi, K. Yase, M. Masuda, T. Shimizu, *Langmuir* **1998**, *14*, 4978–4986.
- [11] J.-H. Fuhrhop, W. Helfrich, *Chem. Rev.* **1993**, *93*, 1565–1582.
- [12] F. M. Menger, S. J. Lee, *J. Am. Chem. Soc.* **1994**, *116*, 5987–5988.
- [13] C. F. v. Nostrum, R. J. M. Nolte, *Chem. Commun.* **1996**, 2385–2392.
- [14] T. Shimizu, M. Masuda, *J. Am. Chem. Soc.* **1997**, *119*, 2812–2818.
- [15] T. Shimizu, M. Kogiso, M. Masuda, *Nature* **1996**, *383*, 487–488.
- [16] T. Shimizu, M. Kogiso, M. Masuda, *J. Am. Chem. Soc.* **1997**, *119*, 6209–6210.
- [17] T. Shimizu, M. Masuda, M. Kogiso, M. Asakawa, *Kobunshi Ronbunshu* **1997**, *54*, 815–828.
- [18] M. Kogiso, M. Masuda, T. Shimizu, *Supramol. Chem.* **1998**, in press.
- [19] J. H. Dumbleton, T. R. Lomer, *Acta. Crystallogr.* **1965**, *19*, 301–307.
- [20] J.-H. Fuhrhop, J. Koenig in *Membranes and Molecular Assemblies: The Synkinetic Approach*, The Royal Society of Chemistry, Cambridge, **1994**, p. 186.
- [21] A. Tardieu, V. Luzzati, *J. Mol. Biol.* **1973**, *75*, 711–733.

## A New Look at the Diels–Alder Transition State\*\*

Claude Spino,\* Marc Pesant, and Yves Dory\*

In relation to the unexpectedly high reactivity of 2-carbomethoxy-1,3-butadiene (**1**) in Diels–Alder reactions (Scheme 1), we recently suggested the presence of a strong



Scheme 1. Dimerization of **1**. The reaction is fast at or below room temperature.

double-bond character between C2 and C3 in the transition state (TS).<sup>[1]</sup> To gain better insight into the mechanism of the Diels–Alder reaction, we reconstructed the whole butadiene–ethylene reaction pathway by means of the intrinsic reaction coordinate (IRC) approach.<sup>[2]</sup> Then, selected structures were extracted to obtain their orbitals, geometries, and energies. We were surprised to witness that the various orbital interactions do not occur simultaneously during the Diels–Alder reaction. The four-electron interaction of symmetric orbitals (Figure 1, green and red curves) begins well in advance at a distance of over 3.0 Å between the diene and dienophile.<sup>[3]</sup> By comparison the two-electron interaction between the antisymmetric orbitals (blue curve) commences at a distance near 2.4 Å! The reason behind this chronology is not yet clear. Remarkably though, many of the geometrical features observed in most (if not all) calculated concerted TS (Scheme 2) of the ethylene–butadiene reaction (and indeed of other systems) reflect perfectly this asynchronicity of molecular orbital interactions.<sup>[4]</sup> Shorter C2–C3 and longer C5–C6 bonds reflect an advanced HOMO<sub>dienophile</sub>–LUMO<sub>diene</sub> interaction, while short C1–C2/C3–C4 and long forming  $\sigma$  bonds are indicative of an emerging HOMO<sub>diene</sub>–LUMO<sub>dienophile</sub> interaction.<sup>[3]</sup> In effect, the long  $\sigma$  bonds reflect an early TS, while the well-developed C2–C3  $\pi$  bond is reminiscent of a late TS, as we suggested earlier.<sup>[1]</sup>

Fukui's frontier molecular orbital (FMO) theory<sup>[5]</sup> has proved to be a valuable tool in predicting the rate and selectivity of organic reactions, in particular pericyclic reactions and cycloadditions.<sup>[6]</sup> This principle was used to predict

[\*] Prof. C. Spino, Prof. Y. Dory, M. Pesant  
Université de Sherbrooke  
Département de Chimie  
Sherbrooke, Qc, J1 K 2R1 (Canada)  
Fax: (+1) 819-821-8017  
E-mail: cspino@courrier.usherb.ca  
ydory@aix1.si.usherb.ca

[\*\*] We thank Prof. Jean Lessard for useful discussions. We acknowledge the Natural Sciences and Engineering Council of Canada for financial support. We thank Brett Bode for his great software MacMolPlt, which was used to display the orbital drawings of Figure 1.

Supporting information for this article is available on the WWW under <http://www.wiley-vch.de/home/angewandte/> or from the author.